RSC Advances

ROYAL SOCIETY OF CHEMISTRY

www.rsc.org/advances

ARTICLE TYPE www.rsc.org/xxxxxx | XXXXXXXX

Amorphous Carbon Layer Contributing Li Storage Capacity to Nb_2O_5@C Nanosheets

Lei Wang,[a] Boyang Ruan,[b] Jiantie Xu,[b] Hua Kun Liu[b,*] and Jianmin Ma[a,b,*]

Received (in XXX, XXX) Xth XXXXXXXXX 200X, Accepted Xth XXXXXXXXX 200X
First published on the web Xth XXXXXXXXX 200X
DOI: 10.1039/b000000x

In this work, amorphous carbon very thin layers coated on Nb_2O_5 nanosheets flexible composite have been successfully synthesized. The composite delivers a discharge capacity of 396 mAh g^{-1} after 100 cycles at a current density of 100 mA g^{-1}, which is very much higher than for bare Nb_2O_5 nanosheets.

Lithium-ion batteries (LIBs) have achieved successful applications in portable electronics and become promising power sources in transportation.[1, 2] As one of the most important anodes in commercial LIBs, graphite has limited the development of safe and high-capacity batteries, due to its low charge-discharge plateau and low theoretical capacity (374 mAh g^{-1}). In the past several years, nanostructured transition metal oxides (Fe_2O_3, Fe_3O_4, MnO, SnO_2, NiO, Co_3O_4, CuO, etc.) have received intensive attention due to their high charge/discharge capacity and higher discharge plateau compared to graphite.[3-10] Most of these materials, however, suffer from volume change during charge/discharge processes, which is detrimental to their cycle life. Thus, it is still a challenge to explore high-capacity, stable anode for advanced LIBs.

In the early 1980s, Reichman and Bard reported the feasible application of Nb_2O_5 as a cathode in nonaqueous lithium cells.[11] Recently, orthorhombic Nb_2O_5 (T-Nb_2O_5) has been reported to be an intercalation pseudocapacitive material, with a crystalline network which offers two-dimensional transport pathways and little structural change on intercalation.[12] This intercalation facilitates charge storage within short periods of time. Inspired by the lithium-intercalation characteristics of T-Nb_2O_5, many groups have investigated the synthesis and electrochemical behaviour of Nb_2O_5 materials. A series of Nb_2O_5 nanostructures have been obtained, including nanofibers,[13] nanotrees,[14] nanotube arrays,[15] nanowires,[16] nanobelts,[17] nanorods,[18] hollow nanospheres,[19] microspheres,[20] nanosheets/nanoflakes,[21, 22] etc.

The lithium storage properties of Nb_2O_5-based electrode, have been intrinsically limited by its poor electrical conductivity ($\sigma \approx 3 \times 10^{-6}$ S cm^{-1}) and slow ion diffusion, which results in low rate performance.[23] To address this question, many efforts have been focused on the synthesis of Nb_2O_5/carbon hybrid materials incorporating various types of carbon (carbon nanotubes, graphene, and other carbon materials) to enhance their electrochemical performance.[24-27] Recently, our group found that an amorphous carbon coating layer can effectively enhance the capacity, cycle life, and rate performance of electrode materials, in which the amorphous carbon layer not only improved the electronic conductivity of the electrode material, but also contributed to high capacity.[28, 29] First-principles calculations indicated that the presence of defects would facilitate the adsorption and diffusion of lithium on defective graphene, and even provide a high capacity of about 1675 mAh g^{-1}.[30-32] In addition, Nishidate and Hasegawa studied the possibilities for the diffusion and accumulation of lithium on defective single-wall carbon nanotubes (SWNTs) using density-functional theory.[33] Kotakoski et al. reported that their amorphous carbon membrane consisted of multivacancy structures constructed of rotated hexagons and other polygons, and could be considered to be defective graphene.[34] Recently, our group synthesized NbO_x@C nanoparticles through oleyamine-assisted hydrothermal method followed by calcination.[35] The NbO_x@C nanoparticles, which were composed of $NbO_{2.432}$ and Nb_2O_5, displayed a discharge capacity of about 298 mAh/g after 200 cycles at 100 mA/g. In this work, we have realized high-capacity Nb_2O_5 nanosheets through coating them with ultrathin amorphous carbon layers, and found that Nb_2O_5@C nanosheets could deliver a discharge capacity of 396 mAh g^{-1} after 100 cycles at a current density of 100 mA g^{-1}, which is very much higher than for bare Nb_2O_5 nanosheets.

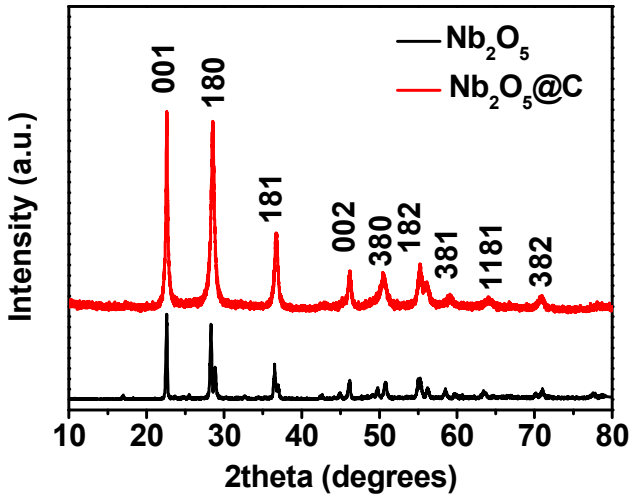

Fig. 1 XRD patterns of Nb_2O_5 nanosheets and Nb_2O_5@C nanosheets.

The Nb_2O_5 nanosheets in the present work were firstly synthesized by the solvothermal method with ethylenediamine (en) as both the alkaline source and the solvent. After immersion in oleic acid, the Nb_2O_5 nanosheets were transformed into Nb_2O_5@C nanosheets, by carbonization of

the oleic acid on the surfaces of the Nb_2O_5 nanosheets. The carbon content in the Nb_2O_5@C sample was confirmed to about 8.1 % by thermogravimetric analysis (TGA) (Fig. S1 in the Supporting Information (S)). In addition, the crystalline phase of Nb_2O_5 after carbon coating was almost unchanged, although the intensity of the peaks obviously increases owing to the heat-treatment at high temperature. Both the Nb_2O_5 nanosheets and the Nb_2O_5@C nanosheets could be well indexed to the peaks of orthorhombic Nb_2O_5 according to the standard card (JCPDS No. 27-1003).

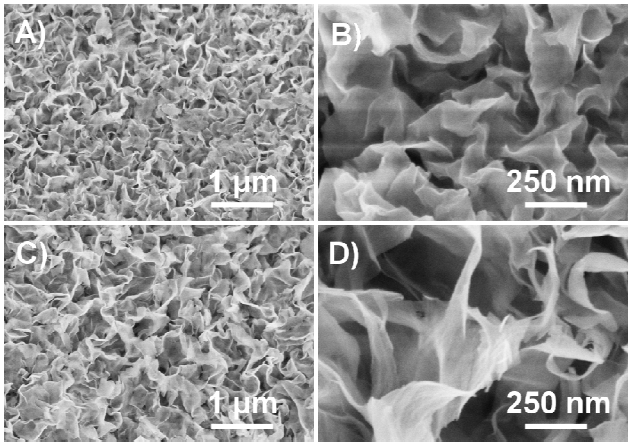

Fig. 2 (A and B) SEM images of Nb_2O_5 nanosheets; (C and D) SEM images of Nb_2O_5@C nanosheets.

The shape and morphology of the Nb_2O_5 nanosheets and Nb_2O_5@C nanosheets were further characterized by scanning and transmission electron microscopy (SEM and TEM). Fig. 2A and B presents SEM images of the as-synthesized Nb_2O_5 nanosheets. As shown in Fig. 2B, the nanosheets are flexible. In this work, we found that our method is highly repeatable, and there is also an important effect on the morphology of the final products from using different ratios of en to distilled water (Figs. S2-S5). Herein, the en might play an important role as a structure-directing reagent. After the coating treatment, the shape of the Nb_2O_5@C nanosheets remained the same, as shown in Fig. 2C and D. This is because the coating layer is extremely thin, which is an important feature of our method. [28-30]

The TEM images give further detailed information on the Nb_2O_5 nanosheets (Fig. 3A and B) and the Nb_2O_5@C nanosheets (Fig. 3C and D). As shown in Fig. 3A and C, both the Nb_2O_5 nanosheets and the Nb_2O_5@C nanosheets are several nanometers thick. As shown in Fig. 3B, the distance between layers is measured to be 0.42 nm, which is in agreement with the lattice spacing of (001) crystalline planes (001). It was reported that the interspaces between the (001) planes provide natural pathways for lithium-ion transport throughout the *ab*-plane with low energy barriers.[12] In addition, as pointed out before, the en could structurally direct the growth of Nb_2O_5 nanosheets along the [001] direction,[12] which might be due to the strong hydrogen bonding between en and the oxygen atoms on the (001) planes, hindering the growth of Nb_2O_5 along other directions. The TEM image in Fig. 3D clearly indicates the presence of single or double amorphous carbon layers. The formation of single or double carbon layers can be attributed to the carbonization of oleic acid molecula adsorbed on the surfaces of the Nb_2O_5 nanosheets. Owing to the rich pathways and amorphous carbon layer, the Nb_2O_5@C nanosheets are expected to have superior electrochemical behavior towards lithium storage.

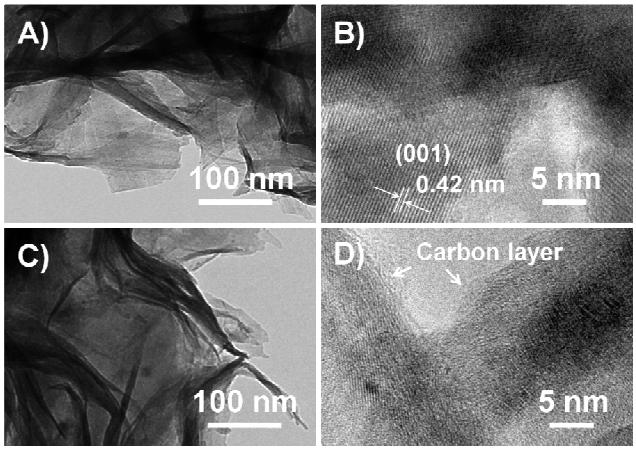

Fig. 3 (A and B) TEM images of Nb_2O_5 nanosheets; (C and D) TEM images of Nb_2O_5@C nanosheets.

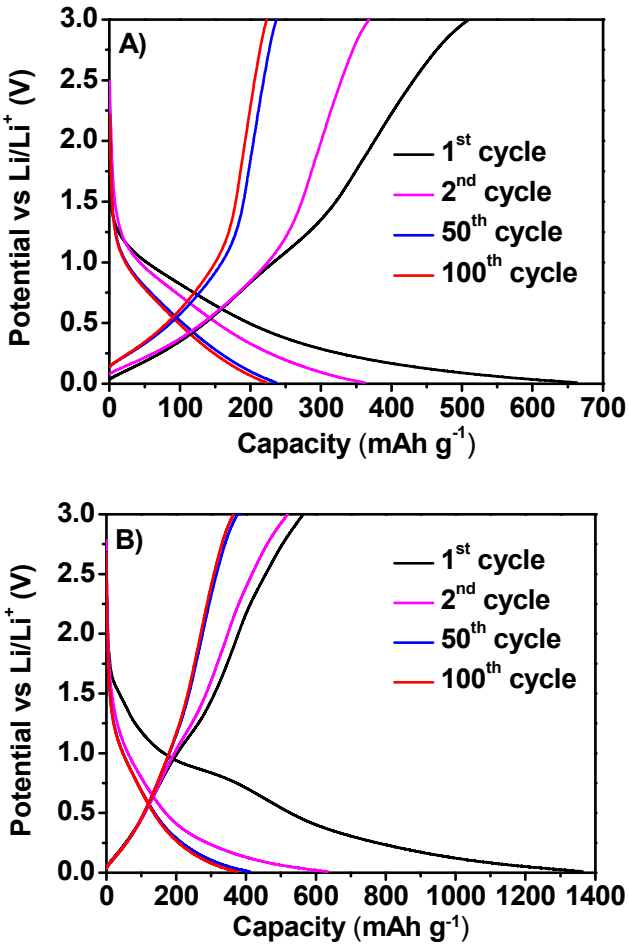

Fig. 4 Discharge/charge curves of (a) Nb_2O_5 nanosheets and (b) Nb_2O_5@C nanosheets for selected cycles at 100 mA g^{-1}.

Standard half-cells were assembled to further investigate

the electrochemical properties of the Nb_2O_5 and Nb_2O_5@C anodes. Galvanostatic charge–discharge cycling, cycling stability measurements, and rate capability tests were conducted to investigate the lithium storage properties. Fig. 4 displays charge–discharge curves of the Nb_2O_5 and Nb_2O_5@C electrodes for the 1st, 2nd, 50th, and 100th cycles at a current density of 100 mA g^{-1}. The typical sloped curves for both the Nb_2O_5 nanosheets (Fig. 4A) and the Nb_2O_5@C nanosheets (Fig. 4B) indicate the intercalation-type electrochemical reaction and that the intercalation of Li^+ into Nb_2O_5 and Nb_2O_5@C electrodes remains a single-phase process. There was no biphasic interface formation during the entire charge-discharge process, which could be verified by the lack of a constant cell voltage plateau.[13] In the first charge-discharge process, the discharge and the reversible capacity of the Nb_2O_5 electrode was 662.7 mA g^{-1} and 509.5 mA g^{-1}, respectively, while the Nb_2O_5@C electrode could present a capacity of 1363.8 mA g^{-1} in discharge and a reversible capacity of 563.4 mA g^{-1}, as shown in Fig. 4. In summary, the Nb_2O_5@C exhibits extra capacity compared to the pure Nb_2O_5 electrode.

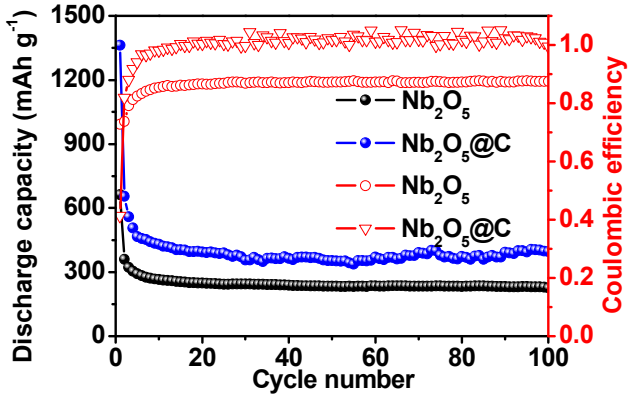

Fig. 5 Cycling performance of Nb_2O_5 nanosheets and Nb_2O_5@C nanosheets at 100 mA g^{-1}.

A highly reversible and stable cycling performance is one of the most important factors in measuring lithium storage properties. Therefore, cycling measurements were conducted to characterize the lithium storage behavior of Nb_2O_5 and Nb_2O_5@C. Fig. 5 shows the cycling performances and coulombic efficiency curves of the synthesized materials at 100 mA g^{-1} in the voltage range of 0–3.0 V. The discharge capacity of the first ten cycles for Nb_2O_5@C and pure Nb_2O_5 both significantly decrease, and then stabilize at 396 mAh g^{-1} and 225 mAh g^{-1}, respectively. From the coulombic efficiency curves, we calculated that the coulombic efficiency of Nb_2O_5@C electrode increases from 41.3% at the first cycle to near 100% after a few cycles, while that of Nb_2O_5 electrode rises from 72.7% at the first cycle to 87.6% after a few cycles.

This work was supported by the National Natural Science Foundation of China (Grant Nos. 51302079) and the Australian Automotive Cooperative Research Centre (CRC-2020). We also thank Dr Tania Silver from Institute for Superconducting and Electronic Materials (University of Wollongong) for revising our manuscript.

The amorphorous carbon layer plays a very important role in improving the electrochemical performance of Nb_2O_5 from the point of view of improving electronic and ionic conductivity, as well as providing high capacity. Compared with pure Nb_2O_5, the presence of carbon efficiently enhances the electronic conductivity and protects the Nb_2O_5 from pulverization, which results in improved rate performance and excellent cyclability.

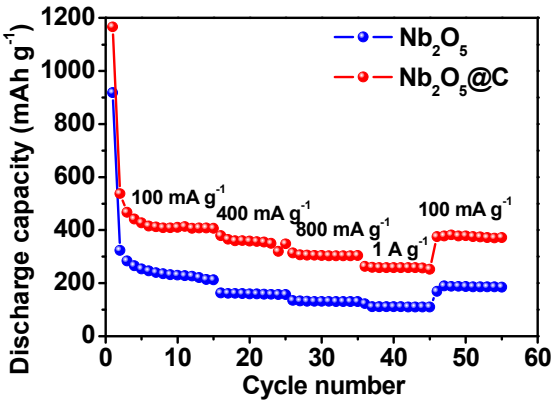

Fig. 6 Rate performance of Nb_2O_5 nanosheets and Nb_2O_5@C nanosheets at various current densities.

Fig. 6 shows the rate capability of the Nb_2O_5 nanosheets and Nb_2O_5@C nanosheets, which indicates a decreasing trend in capacity for both electrodes with increasing current rates. When the current rate gradually increases from low current density (100 mA g^{-1}) to high current density (1 A g^{-1}), the capacity of the Nb_2O_5 and Nb_2O_5@C drops from 209 and 405 mAh g^{-1} to 105 and 250 mAh g^{-1}, respectively. When the current density returns to 100 mA g^{-1}, the specific storage capacity of Nb_2O_5@C reaches 370 mAh g^{-1} for Nb_2O_5@C electrode, however only 186 mAh g^{-1} for Nb_2O_5, as shown in Fig. 6. It is believed that the carbon coating is responsible for the improvement. This Nb_2O_5-carbon structure therefore provides a new design for high-performance Nb_2O_5-based anode materials.

In conclusion, we have successfully synthesized Nb_2O_5 nanosheets by the solvothermal method using en as the alkaline source. The Nb_2O_5@C nanosheets were further obtained through our well-established immersion/annealing techniques involving oleic acid. The as-obtained Nb_2O_5@C nanosheets display a discharge capacity of 396 mAh g^{-1} after 100 cycles at a current density of 100 mA g^{-1} due to their amorphous carbon coating, which could contribute to high lithium storage capacity. The as-obtained Nb_2O_5@C nanosheets are promising for advanced battery application in the future.

Notes and references

[a]*Key Laboratory for Micro-/Nano-Optoelectronic Devices of the Ministry of Education, School of Physics and Microelectronic Science, Hunan University, Changsha 410082, China. E-mail: nanoelechem@hnu.edu.cn (J.M. Ma)*

[b]*Institute for Superconducting and Electronic Materials, University of Wollongong, Wollongong, NSW 2522, Australia Email: hua@uow.edu.au (H.K. Liu)*

† Electronic Supplementary Information (ESI) available: [details of any supplementary information available should be included here]. See DOI: 10.1039/b000000x/

‡ Footnotes should appear here. These might include comments relevant to but not central to the matter under discussion, limited experimental and spectral data, and crystallographic data.

1 K. Smith and C.-Y. Wang, *J. Power Sources*, 2006, **160**, 662–673.
2 B. Scrosati, J. Hassoun and Y.-K. Sun, *Energy Environ. Sci.*, 2011, **4**, 3287–3295.
3 J. M. Ma, J. B. Lian, X. C. Duan, X. D. Liu and W. J. Zheng, *J. Phys. Chem. C*, 2010, **114**, 10671–10676.
4 J. M. Ma and A. Manthiram, *RSC Adv.*, 2012, **2**, 3187–3189.
5 Y. M. Sun, X. L. Hu, W. Luo, F. F. Xia and Y. H. Huang, *Adv. Funct. Mater.*, 2012, **23**, 2436–2444.
6 C. N. He, S. Wu, N. Q. Zhao, C. S. Shi, E. Z. Liu and J. J. Li, *ACS Nano*, 2013, **7**, 4459–4469.
7 Y. H. Xu, G. Q. Jian, M. R. Zachariah and C. S. Wang, *J. Mater. Chem. A*, 2013, 1, 15486–15490.
8 Y. J. Chen, J. M. Ma, Q. H. Li and T. H. Wang, *Nanoscale*, 2013, **5**, 3262–3265.
9 Y. Cai, J. M. Ma and T. H. Wang, *J. Alloys Compd.*, 2014, **582**, 328–333.
10 L. Zhang, H. B. Wu, S. Madhavi, H. H. Hng and X. W. Lou, *J. Am. Chem. Soc*., 2012, **134**, 17388–17391.
11 B. Reichman and A. J. Bard, *J. Electrochem. Soc*., 1981, **128**, 344-346.
12 V. Augustyn, J. Come, M. A. Lowe, J. W. Kim, P.-L. Taberna, S. H. Tolbert, H. D. Abruña, P. Simon and B. Dunn, *Nature Mater.*, 2013, **12**, 518–522.
13 A. L. Viet, M. V. Reddy, R. Jose, B. V. R. Chowdari and S. Ramakrishna, *J. Phys. Chem. C*, 2010, **114**, 664–671.
14 F. Liu and D. F. Xue, *Phys. Scr.* 2010, **2010**, 014074.
15 C. Yan and D. Xue, *Adv. Mater.*, 2008, **20**, 1055–1058.
16 R. Tamang, B. Varghese, S. G. Mhaisalkar, E. S. Tok and C. H. Sow, *Nanotechnology*, 2011, **22**, 115202.
17 X. S. Fang, L. F. Hu, K. F. Huo, B. Gao, L. J. Zhao, M. Y. Liao, P. K. Chu, Y. Bando and D. Golberg, *Adv. Funct. Mater*., 2011, **21**, 3907–3915.
18 B. Varghese, S. C. Haur and C.-T. Lim, *J. Phys. Chem. C*, 2008, **112**, 10008–10012.
19 M. Sasidharan, N. Gunawardhana, M. Yoshio and K. Nakashima, *Mater. Res. Bulletin*, 2012, **47**, 2161–2164.
20 S.-Q. Guo, X. Zhang, Z. Zhou, G.-D. Gao and L. Liu, *J. Mater. Chem. A*, 2014, **2**, 9236–9243.
21 S. Zhuiykov, E. Kats, K. Kalantar-Zadeh and Y. Li, *Nanotechnology, IEEE Transactions on*, 2013, **12**, 13654788.
22 H. Y. Luo, M. D. Wei and K. M. Wei, *Mater. Chem. Phys.*, 2010, **120**, 6–9.
23 X. L. Wang, G. Li, Z. Chen, V. Augustyn, X. M. Ma, G. Wang, B. Dunn and Y. F. Lu, *Adv. Energy Mater.*, 2011, **1**, 1089–1093.
24 E. Lim, H. Kim, C. Jo, J. Chun, K. Ku, S. Kim, H. I. Lee, I.-S. Nam, S. Yoon, K. Kang and J. Lee, *ACS Nano*, 2014, **8**, 8968–8978.
25 G. Li, X. L. Wang and X. M. Ma, *J. Energy Chem*., 2013, **22**, 357–362.
26 A. L. Viet, M. V. Reddy, R. Jose, B. V. R. Chowdari and S. Ramakrishna, *J. Phys. Chem. C*, 2010, **114**, 664–671.
27 L. Y. Wang, L. H. Yu, R. Satish, J. X. Zhu, Q. Y. Yan, M. Srinivasan and Zhichuan Xu, *RSC Adv*., 2014, **4**, 37389–37394.
28 D. N. Lei, T. Yang, B. H. Qu, J. M. Ma, Q. H. Li, L. B. Chen and T. H. Wang, *Sustainable Energy*, 2014, **2**, 1–4.
29 G. Zhou, J. M. Ma and L. B. Chen, *Electrochim. Acta*, 2014, **133**, 93–99.
30 L.-J. Zhou, Z. F. Hou and L.-M. Wu, *J. Phys. Chem. C*, 2012, **116**, 21780-21787.
31 X. F. Fan, W. T. Zheng and J.-L. Kuo, *ACS Appl. Mater. Interfaces*, 2012, **4**, 2432–2438.
32 D. Datta, J. W. Li, N. Koratker and V. B. Shenoy, *Carbon*, 2014, **80**, 305–310.
33 K. Nishidate and M. Hasegawa, *Phys. Rev. B*, 2005, **71**, 245418.
34 J. Kotakoski, A. V. Krasheninnikov, U. Kaiser and J. C. Meyer, *Phys. Rev. Lett.*, 2011, **106**, 105505.
35 Y. Cai, X. Li, L. Wang, H. Y. Gao, Y. N. Zhao and J. M. Ma, *J. Mater. Chem. A*, 2015, **3**, 1396–1399.

Graphic Abstract

Amorphous Carbon Layer Contributing Li Storage Capacity in Nb_2O_5@C Nanosheets

Lei Wang, Boyang Ruan, Jiantie Xu, Hua Kun Liu and Jianmin Ma

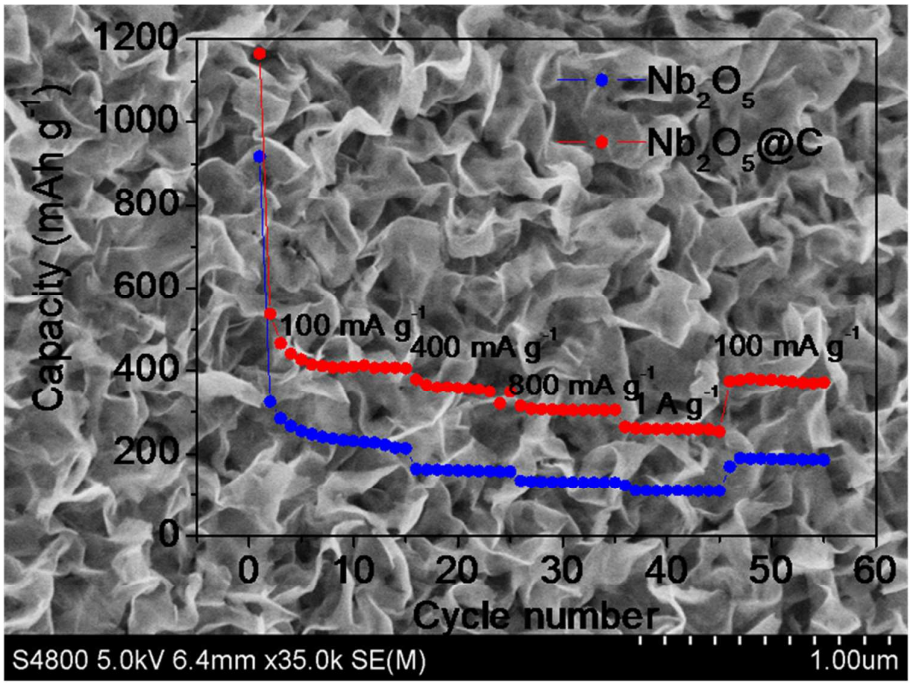

High-capacity of Nb_2O_5 nanosheets have been successfully realized through introducing amorphorous carbon layers, which have been deomonstrated to have a large capacity owing to the existence of defects on amorphous carbon layers.